LEGIBILITY NOTICE

A major purpose of the Technical Information Center is to provide the broadest dissemination possible of information contained in DOE's Research and Development Reports to business, industry, the academic community, and federal, state and local governments.

Although a small portion of this report is not reproducible, it is being made available to expedite the availability of information on the research discussed herein.

LA-UR -83-1416

Conf-830571--2

LA-UR--83-1416

DE83 012785

TITLE: MODELING OF MODIFICATION EXPERIMENTS INVOLVING NEUTRAL-GAS RELEASE

AUTHOR(S) Paul A. Bernhardt
Atmospheric Sciences Group
Earth and Space Sciences Division
Los Alamos National Laboratory
Los Alamos, New Mexico 87545
United States of America

SUBMITTED TO: International Symposium on "Active Experiments in Space"
Alpbach, Austria
May 23-27, 1983

DISCLAIMER

Los Alamos Los Alamos National Laboratory
Los Alamos, New Mexico 87545

MODELING OF MODIFICATION EXPERIMENTS INVOLVING NEUTRAL-GAS RELEASE

Paul A. Bernhardt

Los Alamos National Laboratory
Los Alamos, NM 87545

ABSTRACT

Many experiments involve the injection of neutral gases into the upper atmosphere. Examples are critical velocity experiments, MHD wave generation, ionospheric hole production, plasma striation formation, and ion tracing. Many of these experiments are discussed in other sessions of the Active Experiments Conference. This paper limits its discussion to 1) the modeling of the neutral gas dynamics after injection, 2) subsequent formation of ionosphere holes, and 3) use of such holes as experimental tools.

Keywords: Ionospheric Modification

1. INTRODUCTION

A technique for artificially disturbing the earth's plasma environment involves the release of neutral gas. Once released, some gas species ionize via collisional or photo processes, increasing the plasma concentration. Other species, however, react chemically to neutralize the ambient plasma, decreasing the plasma concentration. Thus, neutral gas releases may be used for controlled perturbation of the ionized atmosphere.

A number of neutral and ion gas dynamics problems are encountered during the analysis of ionospheric modification by neutral gas release. After a vapor is expelled into the rarefied upper atmosphere, it is subject to the effects of condensation, collisional heating, chemical reactions, diffusive transport. The modified plasma regions are influenced by chemistry, microinstabilities, fluid-type gradient instabilities, and ambipolar diffusion.

The objective of this paper is to present an overview of the modeling required to describe ionospheric modification by neutral injection. As examples, chemical releases from the Space Shuttle will be considered. The modeling will be limited to releases which produce plasma holes via chemical reaction. The theories employed, however, should be applicable to a wider range of applications. Following the discussion of how ionospheric holes are formed, their influence on high power radiowaves is described.

2. NEUTRAL GAS DYNAMICS

The chemicals (H_2O, CO_2, N_2, H_2, etc.) found in the rocket exhaust react with O^+ and electrons in the ionosphere to produce neutralization. Consequently, the rocket engines can be used as tools for ionospheric modification (Ref. 1). In this section, the exhaust flow from the Space Shuttle engines is described using the results of gas dynamics theory.

2.1 Condensation in Rocket Exhaust

Condensation droplets may form as a result of the rapid expansion and cooling of the vapors after release. In the condensation process, the latent heat of condensation is liberated. The primary effect of condensation is the removal of molecules from the vapor state. A secondary effect is the increase in the vapor temperature, affecting the rate of gas expansion.

Estimation of the degree of condensation in vapor releases is important for several reasons. First, knowledge of the amount of material which remains in vapor form is necessary to predict the consequences of the release. For example, neutralization of ionospheric plasma involves the chemical reaction of the released gas with O^+ ions in the F-layer. A high degree of condensation reduces the amount of material in vapor form and, consequently, limits the effect on the ionosphere.

Second, the fate of the injected substance is dependent of its physical state. The condensate may fall to low altitudes to be evaporated by radiative and collisional heating. Third, clusters of injected vapor molecules may act as condensation centers for cloud formation.

In the report by Bernhardt et al. (Ref. 2), condensation calculations have been done for the Space Shuttle Main Engine (SSME) and the Space Shuttle Orbital Maneuvering System (OMS) engines.

The degree of condensation is taken to be independent of the number of engines per vehicle. The ambient background pressure was assumed to be 10^{-6} Torr (1.333×10^{-4} NT/m^2) which is typical of the Earth's atmosphere at 200 km altitude. The final condensation will change for different background pressures. The cluster growth process stops because of heating of the exhaust vapor by interaction with the background atmosphere. Higher background pressures (i.e., lower altitudes) reduce the final degrees of vapor condensation.

Table I gives the calculated results for the two engines.

Table I. Exhaust Condensation

Engine	SSME	OMS
Exhaust Species	H_2O, H_2	H_2O, H_2, N_2, CO_2, CO
Mass Fraction of H_2O in Supply	.964	.236
Nozzle Exit:		
Pressure (Torr)	294.7	7.76
Temperature (K)	1278	921
Final Mass Fraction of Condensate (kg/kg)	0.312	0.068
Cluster Radius (10^{-10}m)	56.4	2.02
Standard Deviation in Cluster Radii (10^{-10}m)	3.0	0.3
Cluster Temperature (K)	158.11	100.77

The relatively large exit pressure of the SSME (or HHLV engies) causes over 30% of the exhaust vapor to condense into .0056 micron radius ice clusters. This table illustrates that the amount of material which condenses is dependent on the initial temperature and pressure of the exhaust as it is injected into the atmosphere.

The details of the ice cluster formation and growth process are illustrated in Figures 1-3 for the Space Shuttle Main Engine. The horizontal axis for all figures is the distance (x) from the nozzle exit down the plume. Figure 1 illustrates the supersaturation in the engine plume. The peak supersaturation occurs 69 meters from the nozzle. The homogeneous nucleation quickly reduces the supersaturation and causes a slight pressure increase (condensation shock). The gas temperature is elevated by 30°K at the shock (Figure 2). The condensed vapor forms growing ice clusters which have temperatures greater than the vapor temperature. The average radius of the growing cluster is illustrated in Figure 3. The standard deviation in cluster sizes is also indicated. For exhaust releases at 200 km altitude, the degree of condensation is 31.2% yielding .00564 μ meter clusters.

The amount of material which condenses in a rocket plume is a function of 1) the plume constituents, 2) of the thermodynamic properties (i.e., pressure and temperature) at the nozzle exit, and 3) of the state of the background atmosphere. The condensation process produces submicron clusters. The

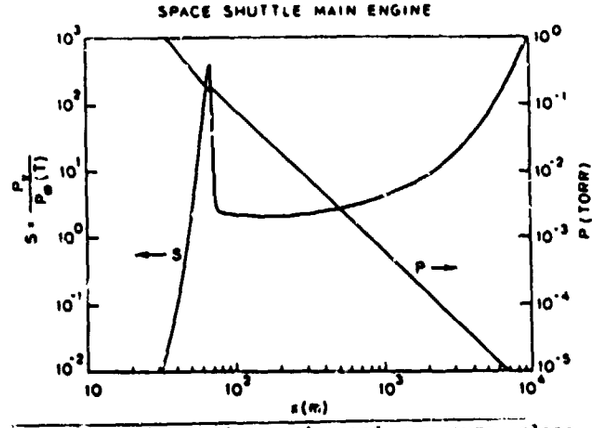

Figure 1. Saturation ratio and pressure along the SSME plume axis.

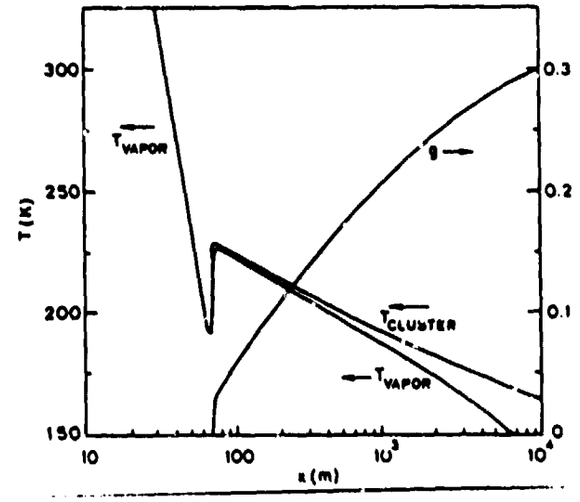

Figure 2. Calculated temperature and degree of condensation along the SSME plume axis.

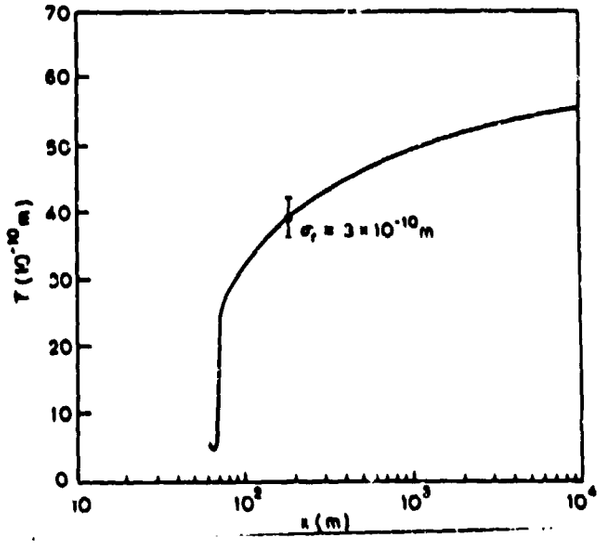

Figure 3. Growth of droplets in the SSME exhaust plume. The standard deviation in droplet size is σ_r.

amount of material which condenses can vary from 0 to 35%.

2.2 Collisional Interaction with Background Atmosphere

The molecules which remain in vapor form are nearly collisionless until they interact with the background atmosphere. A kinetic model of neutral gas flow has been used to model the transition from collisionless to collision ion dominated expansion (Ref. 3).

As an example, consider the flow for the CO_2 component of the Space Shuttle exhaust. The vehicle is moving eastward at 7.7 km/s. The Shuttle engines are oriented downward, ejecting CO_2 with a velocity of 3.1 km/s at a rate of 10^{27} molecules/s. The engines are firing for 10 s, yielding a total release of 10^{28} molecules. The source produces the flow pattern shown in Figure 4 at a time 10.2 s after the start of the burn (0.2 s after the Shuttle engines are turned off). Most of the vapor is in the free-streaming plume 78 km to the east of the start of the burn (Figure 4b). The free-streaming vapor is moving at a high velocity (Figure 4c) and will travel for many tens of kilometers before being collisionally stopped. When the vapor enters a diffusive state, its length will be double that shown in the figure.

2.3 Diffusive Expansion

After the injected gas has thermalized with the background, diffusion governs the expansion. A three-dimensional model has been developed to compute the diffusive expansion of several gases in a multicomponent, nonuniform, chemically-reactive atmosphere (Ref. 4). The diffusion is more rapid at the top of an injected gas cloud because the background atmosphere is less dense at higher altitudes. Consequently, the location of maximum concentration decreases in altitude with time.

An example of the diffusive expansion is shown in Figures 5. A large rocket releasing 2×10^{28} H_2O molecules/second at 400 km altitude travels horizontally at 7.7 km/sec. At time 25.8 seconds after the release, the maximum concentration is 6×10^8 cm^{-3} near 400 km altitude (Figure 5a). One half hour after the release, the maximum concentration is reduced to 3×10^7 cm^{-3}. The altitude of the maximum is 225 km (Figure 5b). The originally circular cross section of the cylindrical cloud become elliptical with a large density gradient on the bottomside.

In most cases, effects of the ionosphere such as ion drag and ion-neutral chemical reactions have negligible effect on the released neutral gas cloud. Consequently, the neutral gas flow can be computed independently of the ion species. The plasma flow and composition, however, is usually dominated by the neutral vapor.

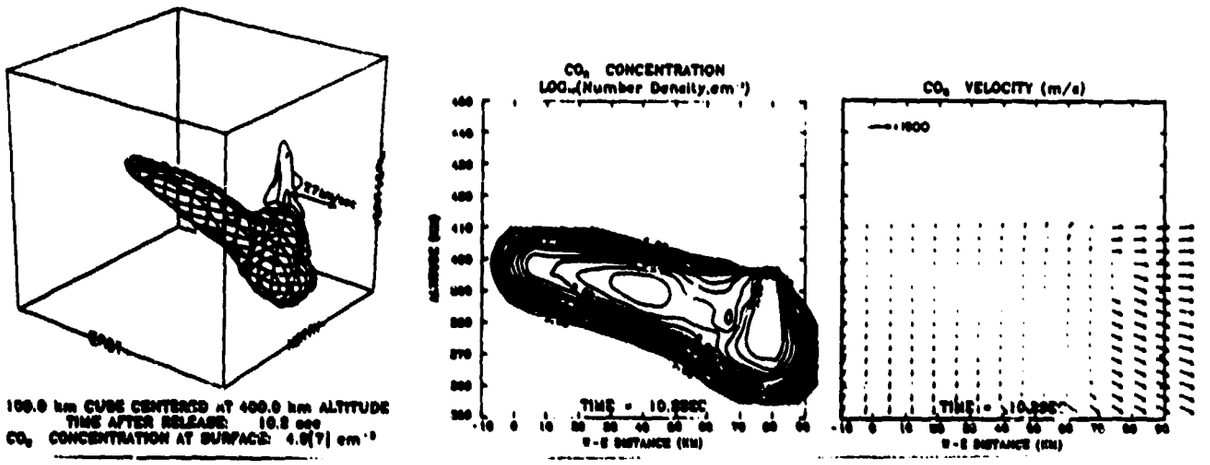

Figure 4. CO_2 exhaust trail produced by the Space Shuttle moving at 7.7 km/s, firing its engines downward with an exhaust velocity of 3.1 km/s. The engines burn for 10 s releasing 10^{27} molecules per second.

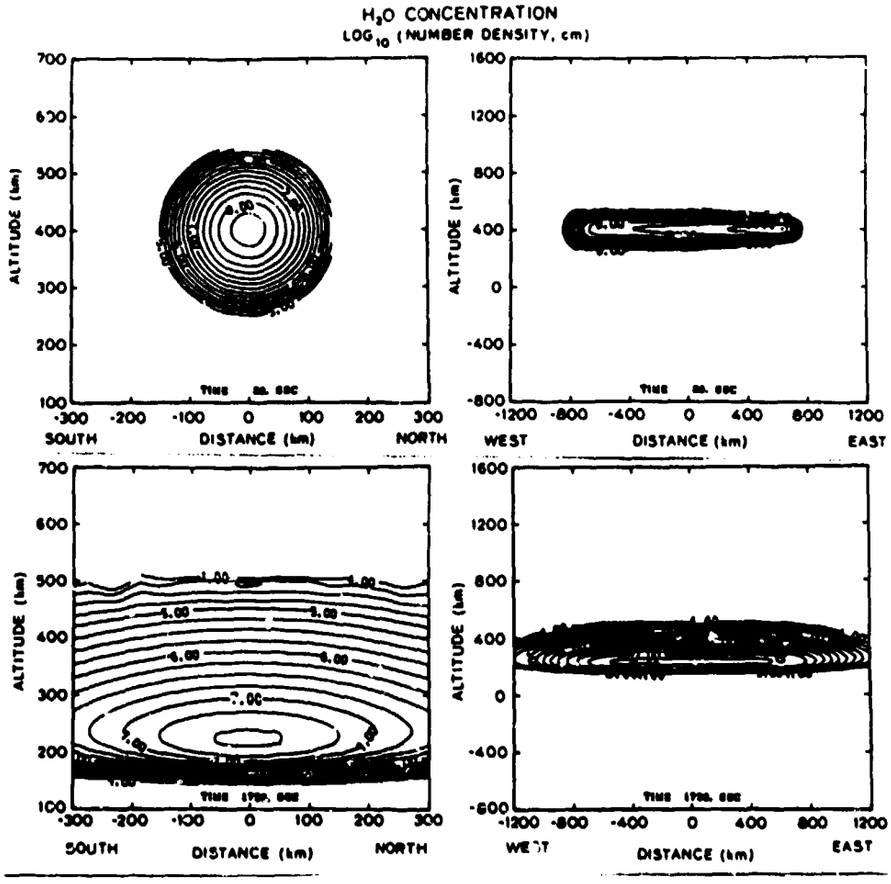

Figure 5. Horizontal burn depositing 4×10^{30} water molecules. Nonuniform diffusion produces apparent settling of the gas cloud.

3. ION GAS DYNAMICS

Polyatomic positive ions such as H_2O^+, O_2^+, NO^+, CN^+ are produced by O^+ reacting with H_2O, CO_2, N_2 and H_2, respectively. These positive ions rapidly react with electrons yielding neutral product species. Polyatomic negative ions such as SF_5^- are produced by electrons reacting with SF_6. The negative ion subsequently reacts with the ambient O^+, yielding neutrals. In all cases, large density gradients in the plasma concentration are formed.

3.1 High ß Dynamics of Negative Ions

The significant chemical reactions stimulated by a SF_6 release into the F-region are listed in Table II (Ref. 5).

Electrons are converted into negative ions which eventually react with O^+ ions to produce neutral species.

As an example, consider the release of SF_6 with orbital velocity at 300 km altitude. For the first few seconds, the neutral SF_6 cloud will move horizontally, unimpeded by the background atmosphere. On the surface of the cloud, electrons will be converted into heavy, negative ions. During the time that the ion-neutral collision frequency is much greater than the ion gyrofrequency, the negative ions will move across the magnetic field.

Results of computations for the negative ion concentration at 0.1, 1.0 and 10.0 seconds after the release of 100 kg of SF_6 is shown in Figure 6. The abscissa on the photo is $z/t - v_s$ where z is distance from the point of release in km, v_s is the injection velocity (7.7 km/sec) and t is time in seconds. The release occurs at 300 km altitude with a background electron and chemistry, ion-electron diffusion and the build up of a plasma layer on the front of the SF_6 cloud. The $SF_5^- + SF_6^-$ ion concentration increases to over a factor of ten above the ambient electron concentration.

Once negative ion clouds are formed, they can produce electric currents and fields which affect their motion. The nature of these effects depends if they are high-ß or low-ß plasma clouds. The ratio of the kinetic energy density to magnetic energy density is

$$\beta = \frac{\frac{1}{2} n_i m (v \sin\alpha)^2}{B^2/2\mu_o}$$

Table II
SF_6 Chemistry for the F-Region

Reaction	Rate
$SF_6 + e^- \rightarrow SF_5^- + F$	$k_1 = \frac{2.2 \times 10^{-7}}{[1 + 1.56 \times 10^{-3} \exp(4770/T)]}$ cm^3/s
$SF_5^- + O^+ \rightarrow SF_5 + O$ or $SF_4 + OF$	$k_2 \sim 5 \times 10^{-8}$ cm^3/s
$SF_6 + O^+ \rightarrow SF_5^+ + OF$	$k_3 = 1.5 \times 10^{-9}$ cm^3/s
$SF_5^+ + e^- \rightarrow SF_4 + F$	$k_4 = 2.0 \times 10^{-7}$ cm^3/s
$SF_5^+ + SF_5^- \rightarrow SF_4 + SF_6$	$k_5 = 4 \times 10^{-8}$ cm^3/s

where n_i = negative ion concentration, m is ion mass, $\underline{v}$ is velocity, α is the angle between $\underline{v}$ and $\underline{B}$, B is magnetic flux density and μ_0 is the magnetic permeability of free space. For the release of SF_6, $m(SF_6^-) = 127$ amu, $v = 7.7$ km/sec, $\alpha = 65^\circ$, and $B = .35$ G. Using these parameters, to have $\beta > 1$ requires then $n_i > 9.4 \times 10^{13}$ ions/m. The calculations give a peak ion concentration of 1.4×10^{13} ions/m^3 which corresponds to $\beta = .15$ for SF_6^-.

A factor of three increase in initial release could yield a high β plasma. The ion cloud motion, for conditions of high β, has been discussed in Ref.(6). The moving plasma cloud builds up electric fields due to charge accumulation at the sides of the cloud. The electric field is perpendicular to the plane containing both the magnetic field vector and the cloud velocity vector at the point of release. The polarization current arising from this electric field accelerates the ambient plasma, a diamagnetic cavity is formed. This disturbance is transmitted along the magnetic field at the Alfvén velocity. At lower altitudes, in the E-region, the electric field produces Pederson and Hall current. Here, momentum is transferred to the neutral atmosphere via ion-neutral collisions. The ion cloud is decelerated as momentum is transferred to the background plasma and neutral atmosphere. Observables include the retardation of the injected cloud and the magnetic field fluctuations which may result from magnetic field fluctuations which may result from currents induced in the ionosphere by the injected cloud.

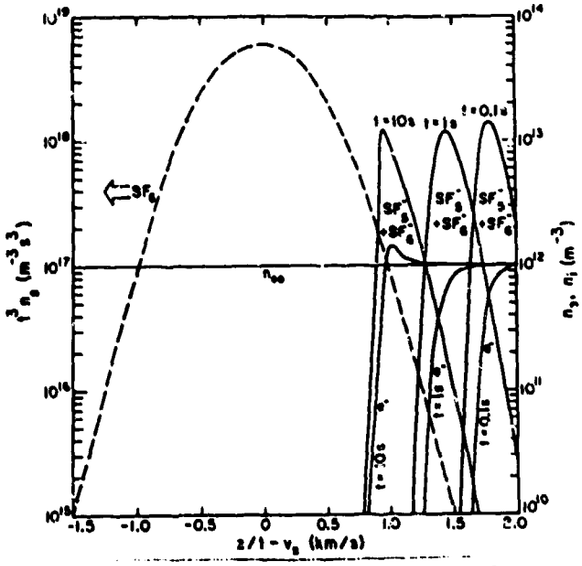

Figure 6. Negative ion concentration, electron concentration and neutral SF_6 concentration relative to a SF_6 cloud moving to the right at 7.7 km/s.

3.2 Plasma Hole Formation

Ionospheric hole formation and recovery has been described in detail in a number of theoretical papers (Refs. 7, 8, 9). The interactions between neutral and ion concentrations, ion velocities, and airglow intensities following a CO_2 release are shown in Figure 7. The diffusing CO_2 gas reacts with O^+ to produce the molecular ion O_2^+. (The molecular ion is denoted by M^+ in the figure.) The O_2^+ and electrons species recombine, neutralizing the plasma. The chemical reactions are:

$$O^+ + CO_2 \rightarrow O_2^+ + CO \qquad \beta_1 = 1.2\times10^{-9} \text{ cm}^3/\text{s}$$

$$O_2^+ + e^- \rightarrow O^* + O^{**} \qquad \alpha_1 = 2.2\times10^{-7}(300/T_e)^{0.8} \text{ cm}^3/\text{s}$$

where T_e is electron temperature. The * indicates excited states of oxygen, $O(^1D)$ and $O(^1S)$, which radiate at 630.0 and 557.7 nm, respectively. The

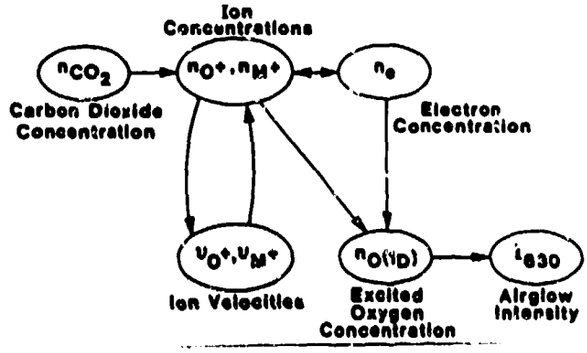

Figure 7. Flow chart describing ionospheric modifications by CO_2 releases.

net effect of a CO_2 release is the reduction of O^+ and electron concentration and the enhancement in the airglow. The recovery of the ionosphere is by plasma transport and, during the day, by photoionization. Under certain conditions, ionospheric holes can stimulate fluid instabilities (Ref. 10). The use of man-made plasma holes for the intensification of high power radiowaves is described in the next section.

4. PLASMA HOLES AND IONOSPHERIC FOCUSED HEATING

Many uses have been found for artificially created ionosperic holes. Diffusive transport is studied by flow into the modified region. The plasma thermal heat balance is upset in the depleted ionosphere producing large enhancements in electron temperature during daytime. Airglow stimulation and quenching is studied by observing optical radiation from species excited by the modification chemistry. Ionospheric holes have been employed to modify currents in the aurora and to seed instabilities at the equator. Some of these topics are discussed in other papers of the Active Experiments Symposium [Refs. 1, 11, 12, 13].

In this section, we present an application which combines ionospheric modification by high power radiowaves with ionospheric modification by neutral gas releases. Existing ground based CW transmitters illuminate the F-region ionosphere with, at most, 100 $\mu W/m^2$. In order to study phenomena such as parametric instabilities, neutral breakdown, and airglow excitation, a new method of beam intensification has been devised. This method is called ionospheric focused heating.

Ionospheric focused heating employs an artificially generated hole in the plasma to act like a convergent lens, focusing the high power radio beam. Simulations of the focusing process have been conducted using computer models previously described in refs. (8,14). The ionospheric hole is formed by releasing 73 kg of CO_2 at 250 km altitude. Chemical reactions between CO_2 molecules, O^+ ions and electrons produce a localized reduction in the plasma concentration.

A 5.19 MHz radio beam with an effective power density of 100 $\mu W/m^2$ launched from the ground by a transmitting antenna having a radiation pattern with a two degree half angle is passed through the ionospheric hole. the resulting perturbation in the electron density is illustrated with contours in Figure 8. The concentration minimum of 4×10^3 electrons/cm^3 is due to the chemical release. The narrow hole in the ionospheric peak at 320 km altitude is the radiowave beam burning through the plasma.

The ionospheric hole produces a factor of 10 increase in the radiowave power density. Contours of logarithmic power density are illustrated in Figure 9. The ionospheric hole produces a well

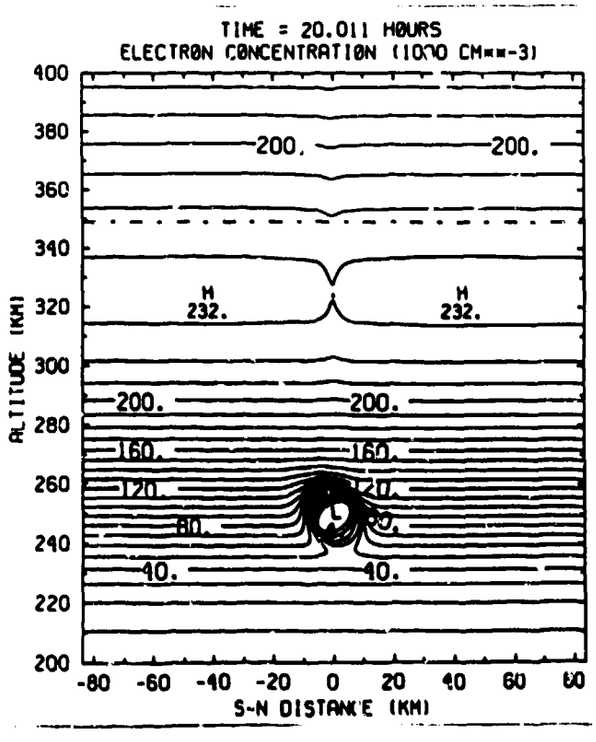

Figure 8. Perturbed electron density contours during ionospheric focused heating.

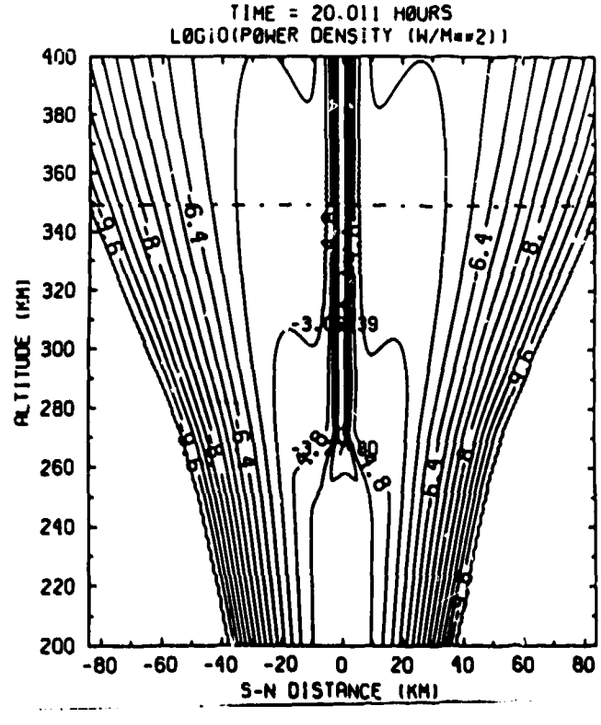

Figure 9. Power density contours in an ionospheric focused radio beam.

formed beam extending from 280 km to above 400 km altitude. The width of the beam is four km. A cross section at 349 km altitude of the focused beam (solid line) is compared with the unfocused beam (dashed line) in Figure 10. Due to limitations in computer memory, only a two dimensional simultation of ionospheric focused heating was conducted. The radiowave and the plasma are assumed to be infinitely extended in the east-west direction. Adding the third dimension to the simulation would have increased the power gain from a factor of 10 to a factor of 100.

Increasing the power density in the radio beam by two orders of magnitude will stimulate new interactions between the high power radiowaves and the space environment. The threshold for the two-plasmon decay instability will be exceeded for the first time. The thresholds for the parametric decay, stimulated Raman, stimulated Brillouin and oscillating two stream instabilities will be exceeded by factors of 100 to 1000. The electron temperature in the ionosphere will be elevated above 10,000 K and the radiowave beam will be outlined in airglow. Under conditions of strong ionospheric focused heating, the neutral breakdown threshold may be exceeded. The ionospheric focused heating experiment may also excite plasma phenomena not previously predicted.

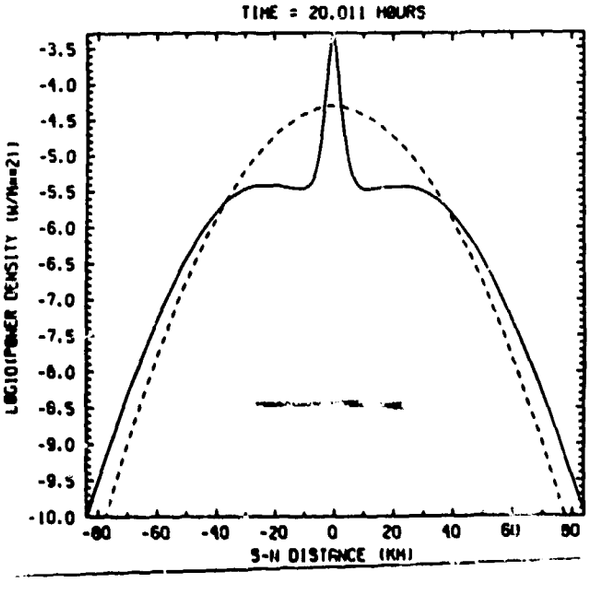

Figure 10. Cross section of an ionospheric focused radio beam.

5. REFERENCES

1. Mendillo M 1983, Rocket exhaust effects as active space plasma experiments of opportunity, Int. Symp. on Active Exp. in Space, Alpbach, Austria.

2. Bernhardt P A, Price, K M and da Rosa A V 1980, Ionospheric modification by rocket effuents, Report ANL/EES-TM-100, Argonne National Laboratory.

3. Bernhardt, P A 1979, High-altitude gas releases: transition from collisionless flow to diffusive flow in a nonuniform atmosphere, J. Geophys. Res., 84 (A8), 4341-4354.

4. Bernhardt P A 1979, Three-dimensional, time-dependent modeling of neutral gas diffusion in a nonuniform, chemically reactive atmosphere, J. Geophys. Res., 84 (A3), 793-802.

5. Bernhardt, P A 1983, Chemistry and dynamics of SF_6 injections into the F-region, submitted to J. Geophys. Res.

6. Scholer M 1970, On the motion of artificial ion clouds in the magnetosphere, Planet. Space Sci., 18, 977-1004.

7. Anderson D N and Bernhardt P A 1978, Modeling the effects of an H_2 gas release on the equatorial ionosphere, J. Geophys. Res. 83 (A10), 4777-4790.

8. Bernhardt, P A 1982, Environmental effects of plasma depletion experiments, Adv. Space Res. 2(3), 129-149.

9. Zinn J, Sutherland C D, Stone S N, Duncan L M, and Behnke R 1982, Ionospheric effects of rocket exhaust products - HEAO-C, Skylab, J. Atm. Terr. Phys. 44 (12), 1143-1171.

10. Bernhardt P A 1982, Plasma, fluid instabilities in ionospheric holes, J. Geophys. Res. 87 (A9), 7535-7549.

11. Narcisi R 1983, Overview of project BIME, Int. Symp. on Active Exp. in Space, Alpbach, Austria.

12. Szuszczewicz E 1983, Project BIME - first results, Int. Symp. on Active Exp. in Space, Alpbach, Austria.

13. Whalen B 1983, Project Waterhole III, Int. Symp. on Active Exp. in Space, Alpbach, Austria.

14. Bernhardt P A and Duncan L M 1982, The feedback-diffraction theory of ionospheric heating, J. Atm. Terr. Phys. 44 (12), 1061-1074.